Supporting Information

Few molecules SERS detection using nanoLens based plasmonic nanostructure: application to point mutation detection

Gobind Das,[1] Salma Alrasheed,[1] Maria Laura Coluccio,[2] Francesco Gentile,[2,3] Annalisa Nicastri,[4] Patrizio Candeloro,[2] Giovanni Cuda,[4] Gerardo Perozziello,[2] and Enzo Di Fabrizio[1]*

[1]Physical Sciences and Engineering (PSE), King Abdullah University of Science and Technology (KAUST), Thuwal 23955-6900, Kingdom of Saudi Arabia

[2]Bio-Nanotechnology and Engineering for Medicine (BIONEM), Department of Experimental and Clinical Medicine, University of Magna Graecia Viale Europa, Germaneto, Catanzaro 88100, Italy

[3]Department of electrical engineering and Information Technology, University of Napoli Federico II - Corso Umberto I 40 - 80138 Napoli

[4]Advanced Research Center on Biochemistry and Molecular Biology, Department of Experimental and Clinical Medicine, University of Magna Graecia Viale Europa, Germaneto, Catanzaro 88100, Italy.

* corresponding author email: gobind.das@kaust.edu.sa

Sections:

Section 1. SERS device with varying nanoLens structure

Various SERS devices with varying nanoLens were realized by combining two techniques: EBL and electroless deposition. Once the structures were written by EBL, the substrate was immersed into HF and metal solution, as described in experimental part. SEM images of various devices with 1-4 nanoLens are reported in **Figure S1** (silver based devices) and in **Figure S2** (gold based devices).

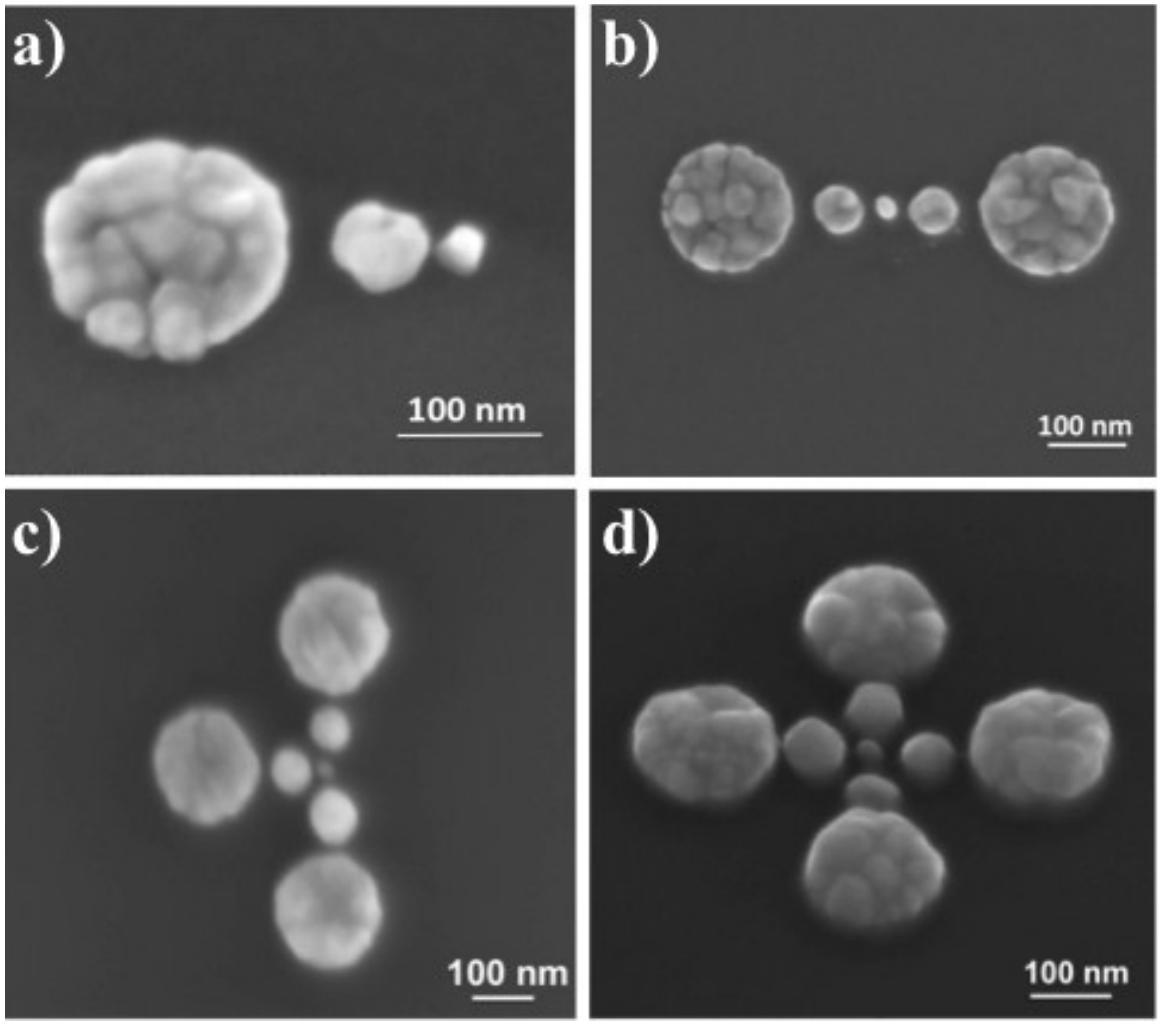

Figure S1: SEM images of SERS device with silver based nanoLens with varying number of nanoLens (N=1-4) (a-d).

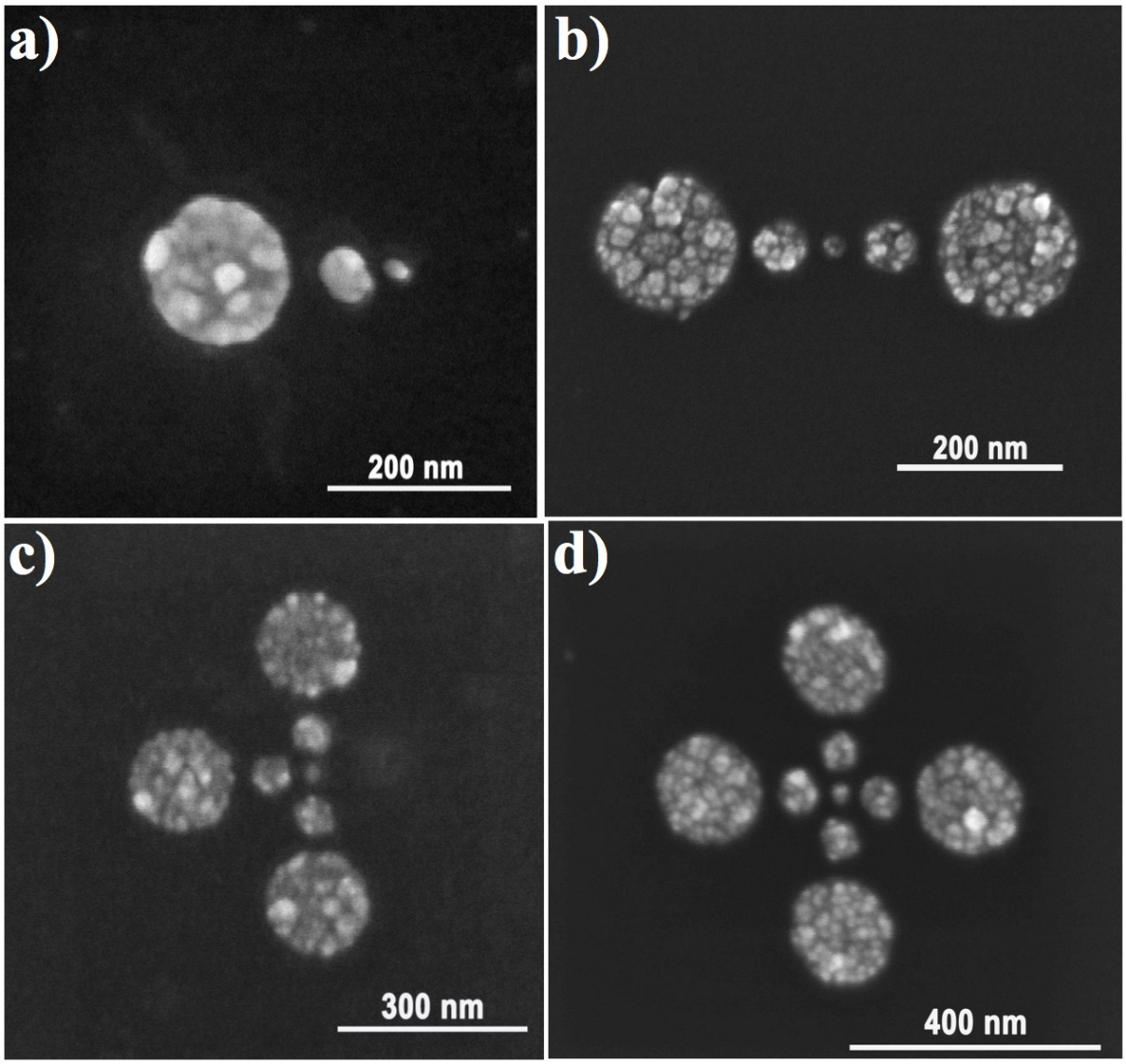

Figure S2: SEM images of SERS device with gold based nanoLens with varying number of nanoLens (N=1-4) (a-d).

Section 2: Calculation of SERS enhancement factor

Rhodamine-6G (Rd6G) fluorescent molecule was chemisorbed over the nanoLens device and over the evaporated silver on Si substrate. SERS spectra of Rd6G on the nanostructure device (red line) and on flat Ag surface (black line) were shown in **Figure S3**. The integration time and the laser power during the measurements were needed much higher than what is required for SSCs nanoLens device in order to attain Rd6G molecule Raman signal.

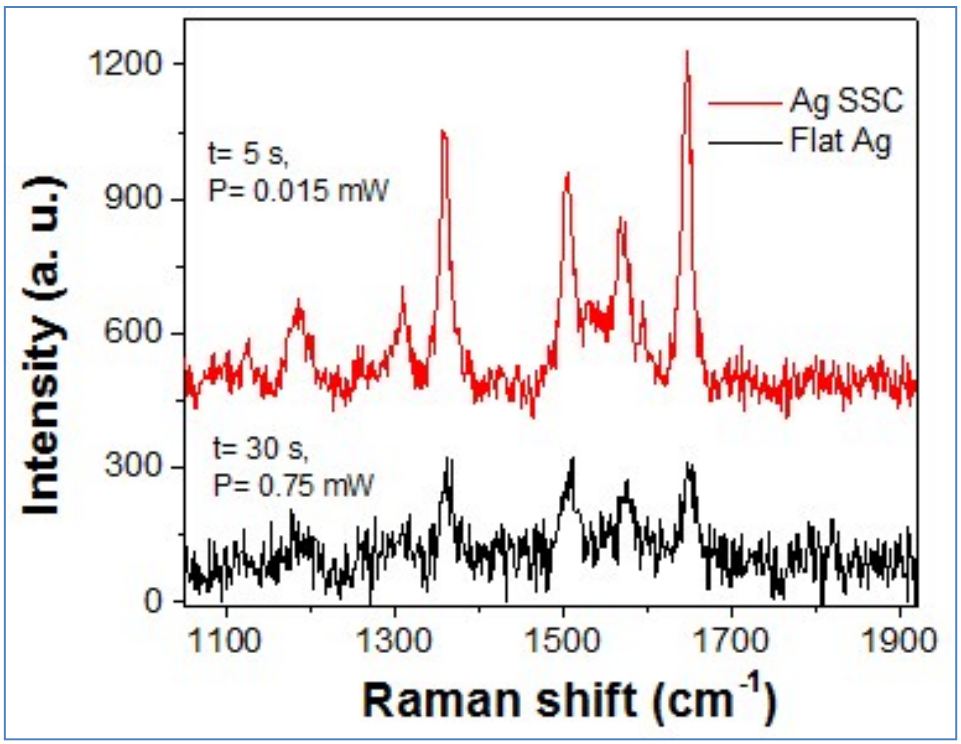

Figure S3: Raman measurements of rhodamine-6G chemisorbed on self-similar chain i.e. nanoLens (red line) and on evaporated silver over Si substrate.

The SERS enhancement factor for nanoLens device with respect to the flat Ag surface can be estimated using the equation:

$$G = \frac{I_{SERS}}{I_{Raman}} * \frac{t_{Raman}}{t_{SERS}} * \frac{A_{Raman}}{A_{SERS}} * \frac{P_{Raman}}{P_{SERS}}$$

where, *I*, *t*, *A* and *P* are Raman intensity, integration time, active Raman area and the laser power, respectively. The subscript, *Raman* and *SERS,* represent the measurement over flat silver deposited on silicon and over nanoLens device, respectively. The active area in case of SERS and Raman measurements is 78.5×10^{-6} and 0.785 μm^2, respectively. Putting all the values, the SERS enhancement factor for nanoLens device is around 1.75×10^7 with respect to the flat Ag evaporated Si substrate.

Section 3: Micro-Raman mapping on devices with varying nanoLens

The SERS devices were designed and then fabricated with varying nanoLens (N=1-4). Rd6G molecules were deposited by means of chemisorption technique over these devices. Micro-Raman mapping measurements were performed on all these devices, keeping all these parameters equal. The mapping analysis was carried out for the Raman band centred at 1650 cm^{-1} for all the four devices with varying number of nanoLens. The mapping analysis reveals the SERS intensity of around 700 for single nanoLens reaches to around 2000 in case of four nanoLens, as shown in **Figure S4**. The summary of the maximum peak intensity is summarized in **Figure 3**.

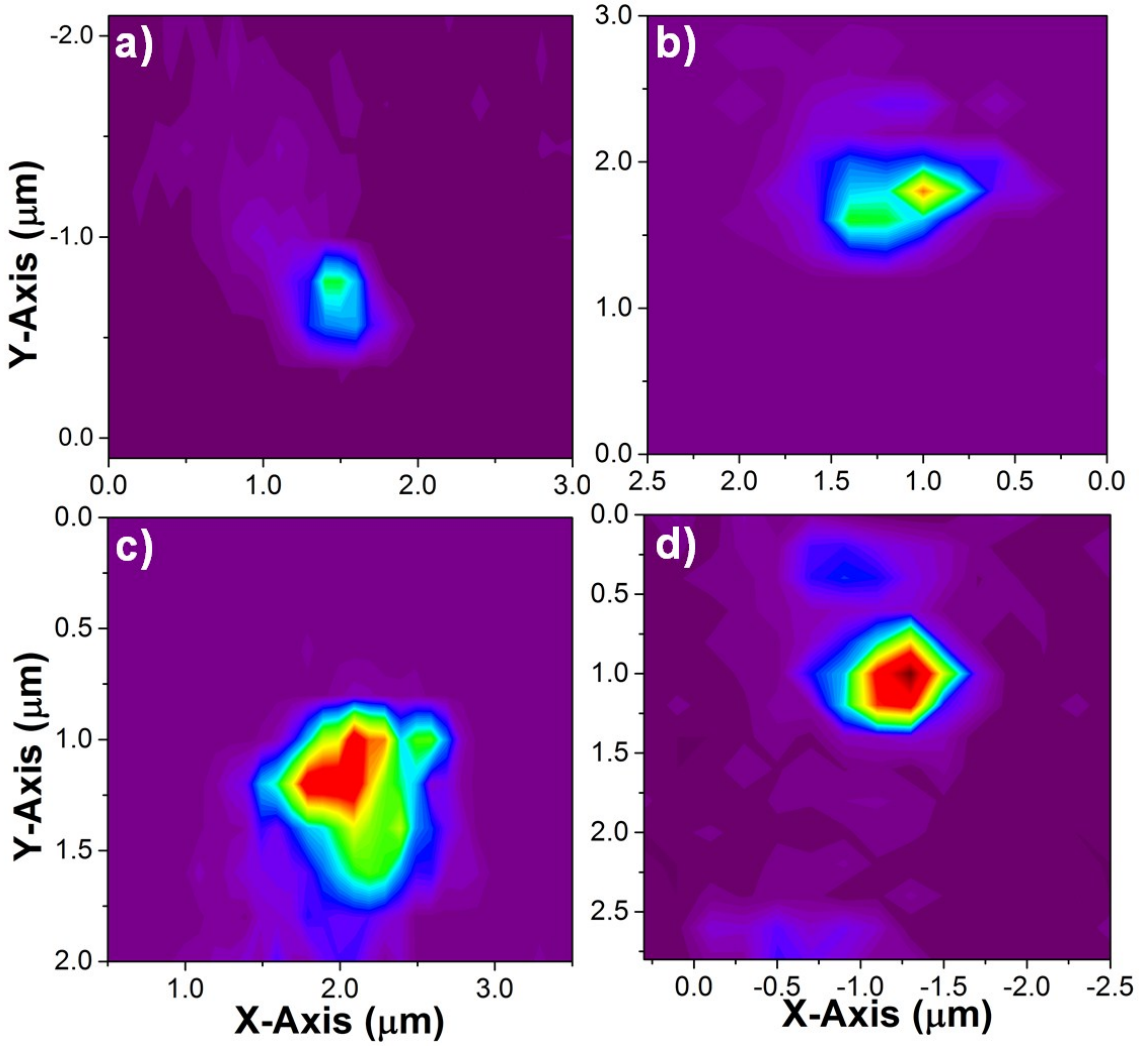

Figure S4: Micro-Raman mapping analysis for rhodamine-6G chemisorbed over 1(a), 2(b), 3(c) and 4 nanoLens (d).

Section 4: Electric field distribution for different plasmonic devices

Theoretical simulations were performed for all the devices (constituting one to four nanoLens), keeping all the parameters same. Electric field distribution for all kinds of nanoLens structures is shown in **Figure S5**. The results suggest the electric field strength for all the devices is close to each other. Since the number of *hot-spot* (and thus the active area) is increased by increasing the number of nanoLens so the SERS signal is increased, as observed in the experimental results.

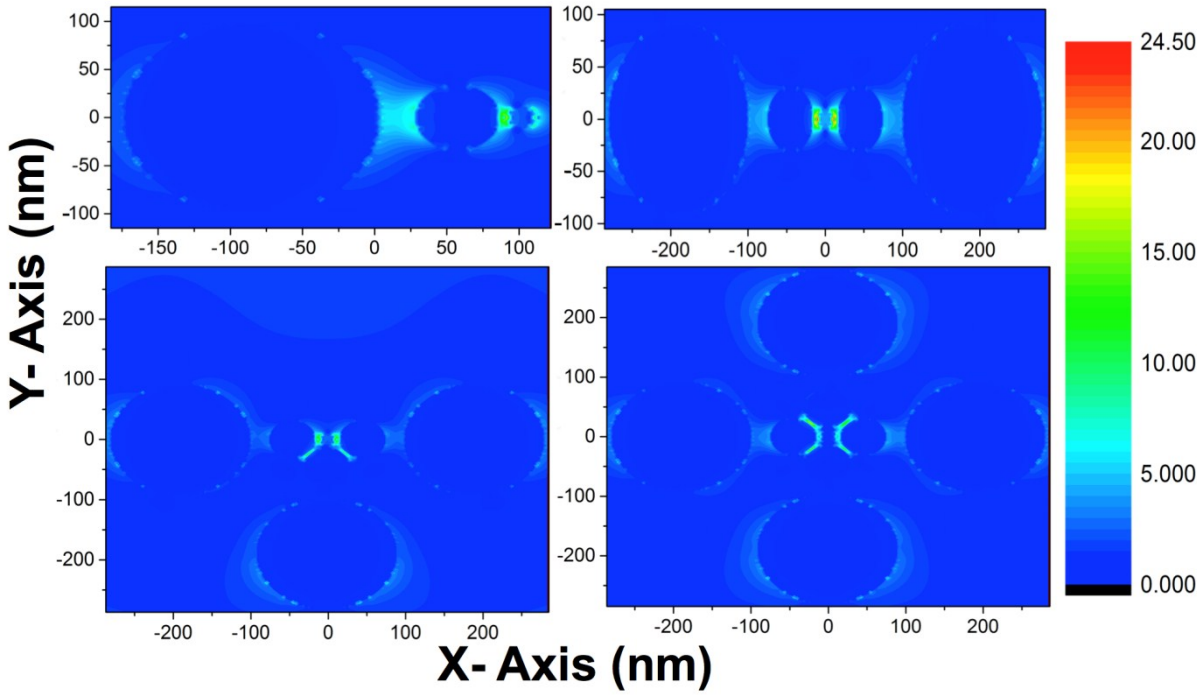

Figure S5: Near field calculation for different devices (one to four nanoLens) (a-d), respectively.

Section 5: Comparative SERS measurements on nanoLens with 2- and 3-NSs

In order to demonstrate the important of fabricating the device with 3- NSs, we carried out the experimental and theoretical studies. For theoretical, the nanostructure design was made with 2- and 3- NSs, keeping all the parameters same for both simulation. The results, shown in the inset, show the presence of 3rd smaller NS creates an intense *hot-spot*. Further confirmation was made with the experimental study. Benzenethiol molecule was deposited over the devices; 2- and 3- NSs device. SERS micro-mapping measurements were carried out on both the devices. In case of 2- NSs substrate, no spectral features were observed while benzenethiol molecular fingerprint spectra were observed. The mapping analysis with the reference band centred at 1584 cm^{-1} shows a clear intense band is observed due to presence of intense *hot-spot* in between two smaller NSs, shown in **Figure S6**.

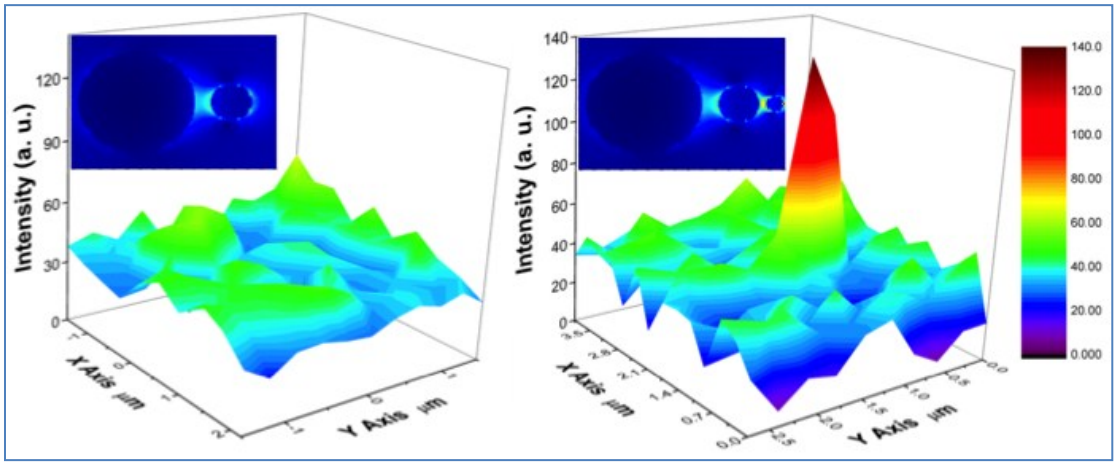

Figure S6: Comparative SERS measurements for benzenethiol deposited over devices with 2- and 3-NSs. In case of 2-NSs, the mapping analysis centred at 1584 cm^{-1} shows the intensity level remains in the noise level whereas in case of 3-NSs, it clearly shows the intensity enhancement due to the creation of *hot-spot* in between 2 smaller NSs. The maximum electric field scale is 19.7 V/m.

Section 6: W1837R peptide of BRCT domain

The BRCA1/BRCT wild type and mutated peptide domain of W1837R were employed for investigating the sensitivity. The peptides were constituted of 16 amino acids. The sequence of the peptide in both cases is listed in **Figure S7**. The amico acid, tryptophan, is replaced by arginine. The mutated site is emphasized in red color and the associated amino acids' structures were also depicted.

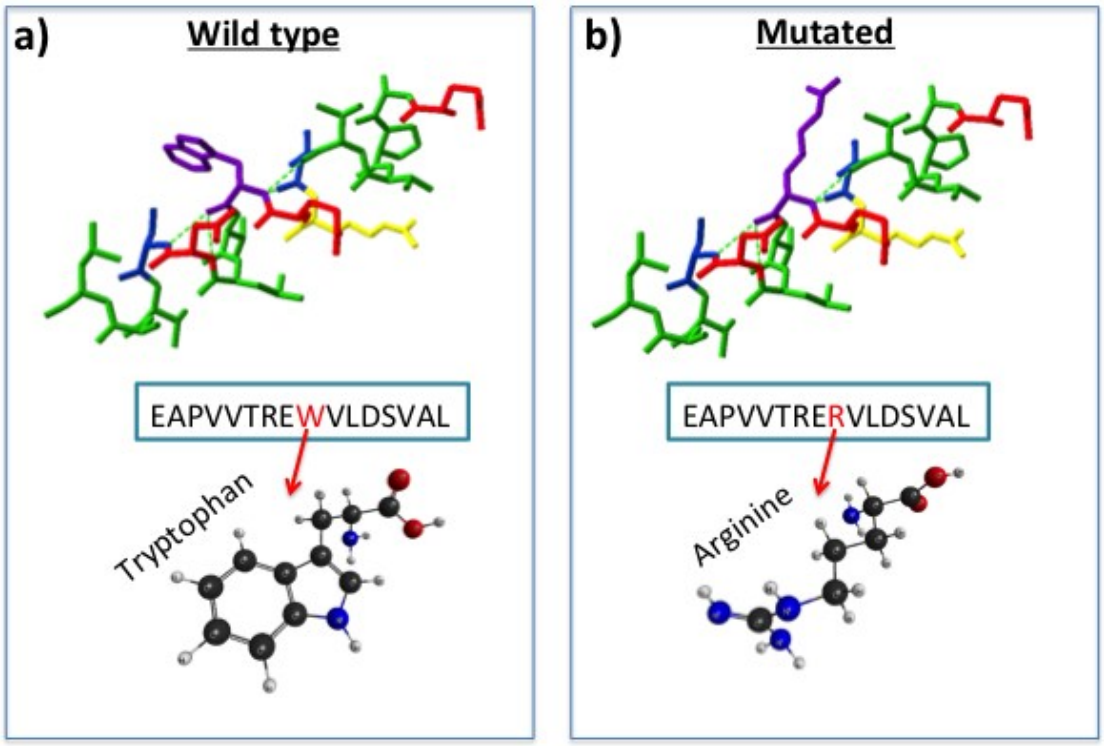

Figure S7: Wild and mutated type BRCA1/BRCT in 3D manner. The 3D design, sequence and the associated amino acid related to the mutation are shown.